Chalcogenide Letters Vol. 5, No. 7, July 2008, p. 143 – 152

OPTICAL PARAMETERS OF ZnSe CHALCOGENIDE NANOSTRUCTURES

Sunil Kumar*, P. Yousaf Khan, N. K.Verma, S. K. Chakarvarti[a]
School of Physics and Materials Science, Thapar University, Patiala – 147004, INDIA
[a]Department of Applied Physics, National Institute of Technology (Deemed University), Kurukshetra – 136119, INDIA

Laser induced time resolved photoluminescence was used to calculate various optical parameters like Einstein's spontaneous coefficients, Einstein's stimulated coefficients, oscillator strengths, dipole moment and integrated cross-section of these chalcogenide nanostructures. ZnSe doped nanoparticles has been fabricated using chemical precipitation method and steric hindrance is given by polyvinylpyrrolidone . The size and morphology of the nanostructures is determined by the XRD, TEM and SAED. ZnSe nanostructures show weak electric dipole visible transitions due to the perturbations of added dopants. These optical parameters are very useful in electronics, computing, optics, biotechnology, medical imaging, medicine, drug delivery, structural materials, aerospace, energy, etc.

(Received June 26, 2008; accepted July 1, 2008)

Keywords: Nanostructures, Photoluminescence, Electric dipole, Excited State lifetime

1. Introduction

Light emission from nanocrystalline phosphors is possible through a radiative recombination process of charge carriers generated by higher energy photon absorption. The colour of the emission can be tailored by changing the crystalline size and appropriate doping. Recently, doped semiconducting nanocrystals (NC) have attracted considerable interest due to their interesting properties such as high luminescence quantum efficiency, short radiative lifetime , size dependent emission color tenability, etc. These materials are considered to be the luminophors for next generation displays, bio-labels, lasers, etc.

A wide variety of spectroscopic techniques have been employed by scientists to probe the static and dynamic processes occurring in complex molecular systems. The generations of extremely short and intense laser pulses have opened the new way for the study of fast transient phenomena such as energy transfer, energy storage, excitation and de-excitation processes in optical materials. A new field of laser spectroscopy is the time-resolved spectroscopic technique in which the detection of these transient phenomena is being done by using short and intense laser pulses. Time- resolved spectroscopy employing laser excitation is a very convenient method for analyzing optical materials in the ultra short time domain. It provides an insight into various atomic and molecular processes, which occur in the materials in the nanosecond and sub-nanosecond time regime. The relaxation parameters associated with various optical transitions reflect the atomic and molecular processes going on in these materials and their environment. Many physical and chemical properties influencing the optical transitions can be investigated by nanosecond time-resolved spectroscopy techniques [1-15]. In 1996, R. M. Park et al. had studied time-resolved luminescence data from heavily nitrogen doped ZnSe. The luminescence exhibited a decay time and a rise time, which increased with decreasing energy of observation. Furthermore, both the decay times and rise times decreased with increasing temperature. These observations are

*Corresponding author: sunilkumar32@gmail.com

consistent with the following model: (i) a band of states was created due to fluctuations in the ionized impurity concentrations; (ii) a portion of the carriers captured by the shallower impurity states were transferred to deeper states prior to recombination. In 2000, J.F. Suyver et al[21]. had studied the luminescence properties of nanocrystalline ZnSe: Mn^{2+} prepared via an inorganic chemical synthesis. Photoluminescence spectra showed distinct ZnSe and Mn^{2+}` related emissions, both of which were excited via the ZnSe host lattice. The Mn^{2+} emission wavelength and the associated luminescence decay time depend on the concentration of Mn^{2+} incorporated in the ZnSe lattice. Temperature-dependent photoluminescence spectra and photoluminescence lifetime measurements were also presented and the results were compared with those of Mn^{2+} in bulk ZnSe. Better results are expected for ZnSe which has a valence band-edge at higher energy with respect to ZnS. In 2005, Changlong Jiang et.al[23]; had studied ZnSe hollow spheres synthesized hydrothermally at 140 °C, by using reducing agent. Both the transverse optic (TO) and longitudinal optics (LO) phonon peaks in the Raman Spectra of the ZnSe showed the obvious shift to lower frequency compared to bulk values, a blue shift has been observed in PL spectra. In 2006, C.X. Shan et. al[24]; had prepared wurtzite ZnSe nanowires on GaAs substrates by a metal-organic chemical vapour deposition system. Electron microscopy showed that they were smooth and uniform in size. Both transmission electron microscopy and x-ray diffraction reveal the wurtzite structure of the nanowires, which grows along the (0001) direction. Raman scattering studies on individual nanowires were performed in the back-scattering geometry at room temperature. Besides the commonly observed longitudinal and transverse optical phonon modes, a possible surface mode located at 233 cm^{-1} is also observed in the Raman spectrum. A peak located at 2.841 eV was clearly observed in the photoluminescence spectra of the nanowires, which can be assigned to near band edge emissions of wurtzite ZnSe. In 2006, S Venkatachalam et al[25]. deposited Zinc selenide (ZnSe) thin films onto well cleaned silicon (100) and glass substrates at different substrate temperatures (483–589 K) using vacuum evaporation method under a vacuum of 4×10^{-3} Pa. The compositions of the deposited films were determined by Rutherford backscattering spectrometry and the percentage of iodine concentration was calculated as (ZnSe) I 0.001. The x-ray diffractograms reveal the cubic structure of the film oriented along the (111) direction. In optical studies, the transition of the deposited film is found to be a direct allowed transition. The optical energy gaps of the deposited films are found to be in the range from 2.72 to 2.60 eV. ZnSe/silicon Schottky diodes were fabricated. From the current–voltage measurement, the ideality factor was found to be in the range 2.01–3.51. From the capacitance–voltage studies, the built in potential was found to be 1.51 V. The values of effective carrier concentration (*N*A) and the barrier height are calculated as 4.37×10^{11} cm^{-3} and 1.95 eV, respectively. Thaddeus J. Norman Jr. et al.[22] had synthesized Cu(II) doped ZnSe nanoparticles using molecular cluster precursors. The Cu(II) dopant had the effect of quenching the ZnSe band edge emission, yet only weak emission from Cu(II) centers was observed. An X-ray Absorption Fine Structure (XAFS) experiment was performed on the Cu(II) doped ZnSe nanoparticles. In this paper optical parameters of ZnSe nanostructures have been calculated using laser induced photoluminescence spectra.

2. Synthesis of ZnSe nanophosphors

Nanophosphors[20-31] were prepared by aqueous colloidal precipitation method at room temperature. The colloidal precipitation technique has been found to have a number of advantages including easy processability at ambient conditions, possibility of doping of different kinds of impurities with high doping concentration even at room temperature, good control over the chemistry of co-doping particularly when different impurities are incorporated simultaneously in the host lattice, easiness of surface capping with a variety of different steps involved in the synthesis process of nanophosphors. Different synthesis methods viz. reverse micelles, homogeneous precipitation and colloidal precipitation, etc. have been carried out by various researchers to prepare the doped nanocrystalline ZnSe phosphors. By comparing properties of the materials obtained from different routes, colloidal precipitation was found to be better for producing efficiently luminescent nanophosphors in terms of process simplicity, effectiveness of

doping and higher yield etc. Different analytical grade chemicals have been purchased from sd-fine Chemicals, India. The synthesis employed co-precipitaton reaction of inorganic precursors of Zn^{2+} and Se^{2-} with dopant ions (Mn^{2+}, Cu^{2+} and Co^{2+}) in aqueous medium containing the capping molecules of 1% PVP prepared by dissolving 1gm of PVP in 100ml of distilled water. The different concentrations of impurities in solution were maintained at (10%, 5%, 1% & 0.1%) with Zn^{2+}, for ZnSe:Mn, ZnSe:Cu, ZnSe:Co samples. 2.195 g of $Zn(ac)_2$ has been dissolved in 50 ml of distilled water to obtain 0.2 M solution. 1.7294 g of Na_2SeO_3 has been dissolved in 50 ml of distilled water to get 0.2 M of solution. In the synthesis of ZnSe, 25ml of $Zn(ac)_2$ solution was mixed with solution of polyvinylpyrrolidone(PVP), the capping agent was added to avoid agglomeration of grown nanoparticles. Nanoparticles with polymer capping were precipitated by slowly adding 25 ml of 0.2 M Na_2SeO_3 solution to the above mixture. A white colloidal suspension was obtained immediately after adding Na_2SeO_3 solution. The precipitates were separated by 2000 rpm centrifugal machine and washed several times with distilled water. Then the sample was dried in a vacuum oven at a temperature of about 80 $_oC$.

3. Morphological characterization

3.1 *X-ray diffraction studies*

X-ray diffraction (XRD) is an efficient tool for the structural analyses and morphological characterization of crystalline materials. In the present studies, XRD patterns have been recorded using D/max-2000 Rigaku (Tokyo) powder X-ray diffractometer using copper characteristic wavelength of 1.5418 Å operated at 40 kV and 40 mA keeping step size (0.02) deg/s. Peak broadening has been observed in recorded diffraction patterns, which show the formation of nanocrystallites. Fig. 1 shows the XRD pattern recorded for pure ZnSe. Comparison of the recorded XRD pattern with standard JCPDS data file 10979 confirms the formation of the wurtzite structure.

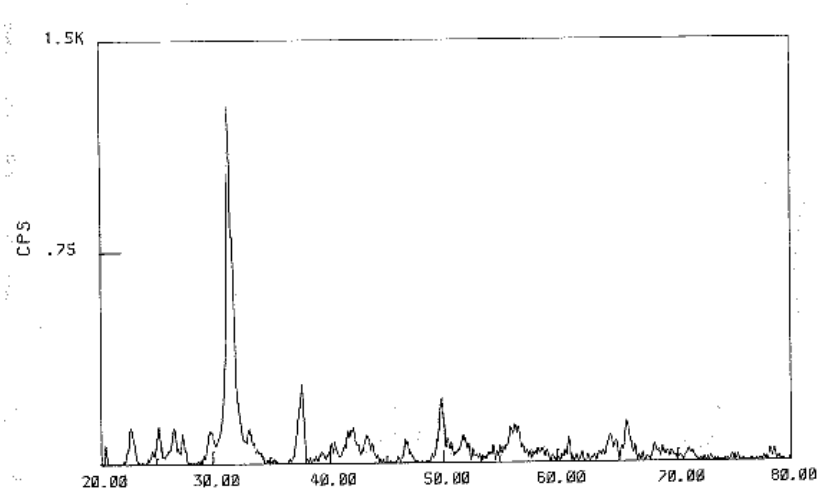

Fig. 1. X-ray diffractogram of the as-synthesized ZnSe nanoparticles.

Average crystallite size has been calculated from the recorded XRD patterns using well known Scherrer Equation:

$$D = 0.89\lambda/\beta \cos\theta$$

where D is the average crystallite size, λ is the wavelength of incident X-ray, β is the full width at half maximum (FWHM) of X-ray diffraction expressed in radian and θ is the position of the diffraction peak in the diffractograms. The mean calculated crystallite size of doped ZnSe nanoparticles is ~14 nm.

3.2 *Transmission electron microscope (TEM) studies*

Electron microscopy is a good tool for the morphological studies of nanomaterials. In the present studies JEOL JEM 2000 Ex. Type TEM was used for recording the electron micrographs. All the micrograph patters were recorded at 80kV and the selected area electron diffraction (SAED) patterns were recorded by keeping camera constant 100cm. Figs. 2 (a) and (b) show the TEM image and SAED pattern for pure ZnSe. It is clear from Fig. 2(a) that all the particles are in nano regime, but the distribution of particles is heterogeneous. Fig. 3 shows the histogram for size distribution of nanoparticles, it is evident from histogram that average particle size is ~14 nm. SAED pattern shown in the fig. 2(b) represents the well defined ring pattern, which confirms the crystalline nature of ZnSe nanoparticles.

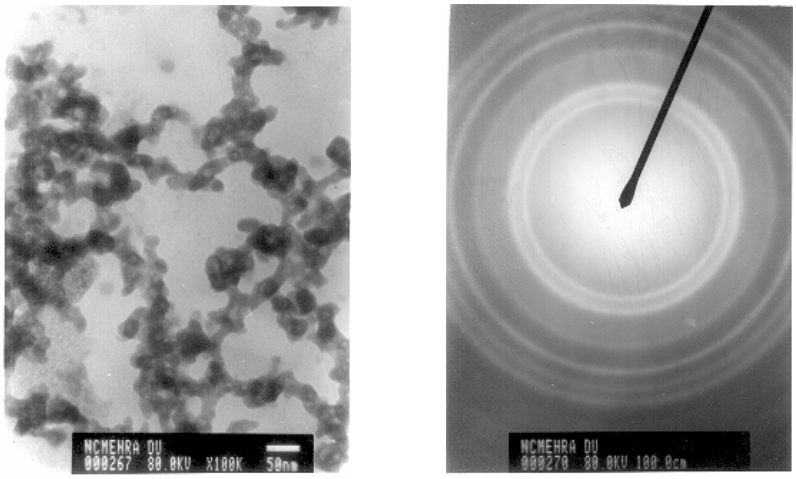

a b

Fig. 2. (a) TEM image of ZnSe (b) SAED pattern for ZnSe nanoparticles

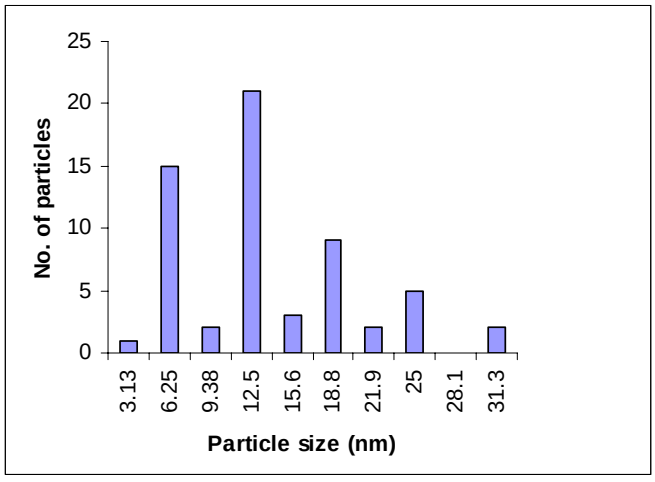

Fig. 3. Histogram of size distribution of ZnSe nanoparticles

4. Photoluminescence studies

For room temperature (300 K) studies, the sample is taken in the form of a powder in a groove specially prepared in a perspex sheet or in the form of a thin film pasted with xylene on a glass plate. Nitrogen laser is the most suitable excitation source (337.1 nm) to irradiate the doped phosphors as laser energy excites the luminescent centers introduced by the dopants in the phosphors very effectively. High photon flux density (10^{19} photons per pulse) of the laser is very useful to excite the short-lived shallow trapping states which otherwise were impossible to excite using conventional light sources like mercury vapor lamp or xenon flash lamp. Short pulse-width of Nitrogen laser (5-7 ns) is helpful to determine the lifetime values accurately in the milli- and micro-seconds time domain without introducing its own effect. The short lived phosphorescence from the sample at an angle of 90° to the incident beam was collected by a fast photomultiplier tube through an assembly of monochromator as a wavelength selective element and glass slab to filter out the UV radiation. The decay signals from the phosphors are recorded by a fast digital type storage oscilloscope, which is interfaced with a computer. Computer simulations are done to calculate lifetime values accurately of the different excited states contributing to the phosphorescence hyperbolic decay.

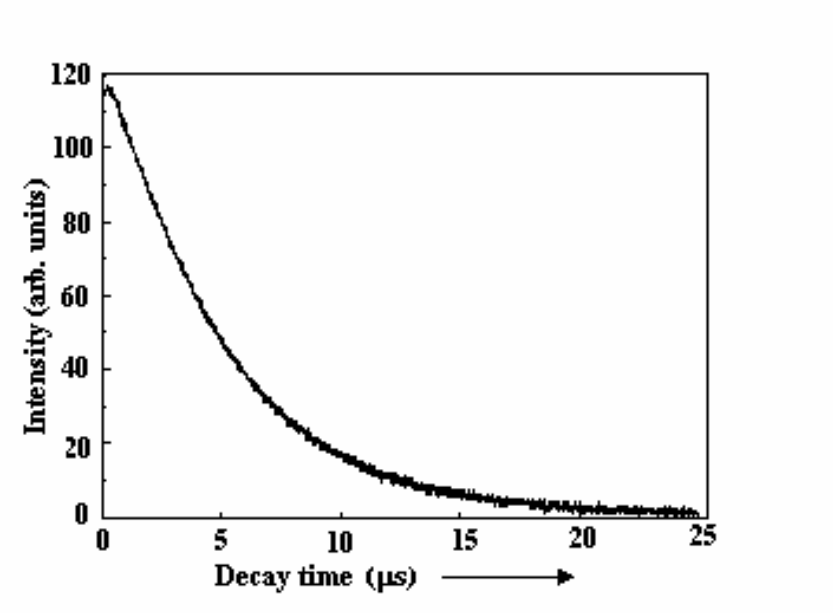

Fig. 4. Hyperbolic type of phosphorescence decay curve for ZnSe:Mn (10%)

If $p_{ed}(ab)$ is the only radiative process from upper level 'a' to the lower level 'b', then $p_{ed} = \tau_R^{-1}$ where τ_R is the emission lifetime of the upper state and p_{ed} is the Einstein's spontaneous coefficient for electric dipole transition.

A dimensionless quantity called the oscillator strength 'f' in case of electric dipole transitions is given by:

$$f_{ed}(\nu) = 1.5 \times 10^4 . \lambda_0^2 . \frac{9}{(n^2+2)^2 . n} \, p_{ed} \qquad (1)$$

where λ_o is the emission wavelength given by c/ν, $p_{ed}(ab) = 1/\tau_R(\nu)$ is transition probability and 'n' is the index of refraction of CaS material. For magnetic dipole transitions the above relation reduces to

$$f_{md} = 1.5 \times 10^4 . \lambda_0^2 . \frac{1}{n^3} p_{md} \quad (2)$$

An electric dipole transition will have a lifetime of 10^{-8} to 10^{-7} second, while a magnetic dipole transition 10^{-3} to 10^{-1} second and a quadruple transition an even longer lifetime..
The spontaneous radiative lifetime is related in simple way to the integrated
Cross section of the transition by the following relation;

$$Ics = \int \sigma d\upsilon = \lambda^2 p/8\pi \quad (3)$$

The relation given below gives the corresponding dipole moment

$$\mu = (3h\varepsilon_o\lambda^3\rho/16\,\pi^3 n)^{1/2} \quad (4)$$

Einstein's Stimulated coefficient is given by following relation

$$B = 2\pi^2\mu^2 / 3n^2\varepsilon_o\, h^2 \quad (5)$$

where μ is the dipole moment of transition from the shallow trapping states of CaS , ε_o is the absolute permittivity of free space, n is the index of refraction and h is Planck`s constant.

The eq. (1) has been used to calculate the oscillator strengths of weak electric dipole transitions while eq. (2) is preferred for calculating the oscillator strengths of the magnetic dipole transitions. The equation (3) has been used to calculate integrated cross section of the transition while equation (4) and (5) are used to calculate the corresponding dipole-moments and Einstein's Stimulated coefficient respectively

The measured values of the transition probabilities for strong transitions at 300 K have been listed in Table-1. The calculated values of trap depth are given in Table-2. The calculated values of the oscillator strengths for different transitions have been shown in Table-3. Further the values of integrated cross-section, Einstein stimulated coefficients and dipole moments are reported in Table-4, 5 and 6 respectively.

Table 1. Excited state lifetime values of pure and doped ZnSe nanophosphors.

Sample No.	Phosphorus impurity(%)	Wavelength (nm)	Einstein's spontaneous coefficients (s^{-1})at 300 K		
			P'	P"	P"'
1	ZnSe	450	0.1607	0.0775	0.0199
2	ZnSe:Mn(10%)	422	0.1466	0.0769	0.0222
	ZnSe:Mn(5.0%)	422	0.1428	0.0578	0.0041
	ZnSe:Mn(1.0%)	407	0.1529	0.0900	0.0347
	ZnSe:Mn(0.1%)	443	0.1488	0.0621	0.0033
3	ZnSe:Cu(10%)	440	0.0806	0.0348	0.0068
	ZnSe:Cu(5.0%)	475	0.2040	0.1694	0.0961
	ZnSe:Cu(1.0%)	440	0.1336	0.0574	0.0147
	ZnSe:Cu(0.1%)	420	0.1358	0.0684	0.0168
4	ZnSe:Co(10%)	449	0.1430	0.0840	0.0214
	ZnSe:Co(5.0%)	427	0.1426	0.0740	0.0193
	ZnSe:Co(1.0%)	475	0.1432	0.0735	0.0188
	ZnSe:Co(0.1%)	456	0.1555	0.0980	0.0261

Table 2. Einstein's Stimulated Coefficient of pure and doped ZnSe nanophosphors recorded at room temperature

S.No	Phosphorus impurity (wt%)	Wavelength (nm)	Einstein's stimulated coefficient $\times 10^{16}$ m^3(rad/s)/(J/s)		
			B'	B"	B"'
1	ZnSe	450(feeble)	6.343	3.059	0.784
2	ZnSe:Mn(10%) ZnSe:Mn(5.0%) ZnSe:Mn(1.0%) ZnSe:Mn(0.1%)	422 422 407 443	4.772 4.647 4.466 5.604	2.503 1.881 2.628 2.338	0.722 0.133 1.012 0.126
3	ZnSe:Cu(10%) ZnSe:Cu(5%) ZnSe:Cu(1%) ZnSe:Cu(0.1%)	440 475 440 420	2.973 9.475 4.930 4.357	1.284 7.865 2.119 2.194	0.254 4.460 0.543 0.541
4	ZnSe:Co(10%) ZnSe:Co(5.0%) ZnSe:Co(1.0%) ZnSe:Co(0.1%)	449 427 475 456	5.606 4.808 6.647 6.365	3.293 2.496 3.412 4.024	0.838 0.651 0.872 1.071

Table 3. Oscillator Strength of pure and doped ZnSe nanophosphors recorded at room temperature

S.No	Phosphor: Impurity(wt%)	Wavelength (nm)	Oscillator strength($\times 10^{-5}$)		
			f'	f"	f"'
1	ZnSe	450(feeble)	3.039	1.465	0.376
2	ZnSe:Mn(10%) ZnSe:Mn (5.0%) ZnSe:Mn(1.0%) ZnSe:Mn(0.1%)	422 422 407 443	2.438 2.375 2.365 2.727	1.279 0.961 1.392 1.138	0.369 0.068 0.536 0.061
3	ZnSe:Cu(10%) ZnSe:Cu(5%) ZnSe:Cu(1%) ZnSe:Cu(0.1%)	440 475 440 420	1.457 4.300 2.415 2.237	0.629 3.569 1.039 1.126	0.124 2.025. 0.266 0.278
4	ZnSe:Co(10%) ZnSe:Co(5.0%) ZnSe:Co(1.0%) ZnSe:Co(0.1%)	449 427 475 456	2.685 2.428 3.017 3.010	1.581 1.260 1.548 1.903	0.402 0.329 0.396 0.506

Table 4. Integrated cross-section of pure and doped ZnSe nanophosphors calculated at room temperature

S.No	Phosphor impurity (wt%)	Wavelength (nm)	Integrated cross-section ($\times 10^{-9}$ m^2s^{-1})		
			I’	I”	I”’
1	ZnSe	450(feeble)	1.294	0.624	0.160
2	ZnSe:Mn(10%) ZnSe:Mn (5.0%) ZnSe:Mn(1.0%) ZnSe:Mn(0.1%)	422 422 407 443	1.038 1.011 1.007 1.161	0.544 0.409 0.593 0.484	0.157 0.029 0.228 0.024
3	ZnSe:Cu(10%) ZnSe:Cu(5%) ZnSe:Cu(1%) ZnSe:Cu(0.1%)	440 475 440 420	0.620 1.831 1.029 0.953	0.268 1.520 0.442 0.480	0.052 0.862 0.113 0.118
4	ZnSe:Co(10%) ZnSe:Co(5.0%) ZnSe:Co(1.0%) ZnSe:Co(0.1%)	449 427 475 456	1.146 1.034 1.285 1.282	0.673 0.536 0.659 0.810	0.171 0.140 0.168 0.215

Table 5. Dipole moment values of pure and doped ZnSe nanophosphors calculated at room temperature

Sample no	Phosphor impurity (wt%)	Wave length (nm)	Dipole – moment values ($\times 10^{-31}$ Cm)		
			μ’	μ”	μ”’
1	ZnSe	450(feeble)	4.645	3.226	1.634
2	ZnSe:Mn(10%) ZnSe:Mn(5.0%) ZnSe:Mn(1.0%) ZnSe:Mn(0.1%)	422 422 407 443	4.029 3.976 3.897 4.366	2.918 2.530 2.990 2.820	1.568 0.674 1.856 0.656
3	ZnSe:Cu(10%) ZnSe:Cu(5%) ZnSe:Cu(1%) ZnSe:Cu(0.1%)	440 475 440 420	3.180 5.677 4.095 3.850	2.090 5.172 2.685 2.732	0.930 3.895 1.360 1.357
4	ZnSe:Co(10%) ZnSe:Co(5.0%) ZnSe:Co(1.0%) ZnSe:Co(0.1%)	449 427 475 456	4.367 4.044 4.755 4.653	3.347 2.913 3.407 3.700	1.689 1.489 1.723 1.909

5. Results and discussion

The optical properties of nano-crystalline semiconductors had been studied extensively in recent years due to their interesting applications suitable for making advanced opto-electronic systems[16-19]. These nanomaterials behave differently from bulk semiconductors due to quantum confinement effect and large surface- to- volume ratio. It was reported that doped nanocrystals of semiconductors can yield high luminescence efficiency. In the present investigation, excited state lifetime measurements of doped ZnSe nanocrystals have been carried out using a pulse excitation method. Hyperbolic decay curves have been observed in case of pure and doped ZnSe nanophosphors with variable concentration of Mn, Cu and Co impurities. Pure exponential components of decay curves were extracted from the hyperbolic decays (Fig. 4) with the help of computer software. The Einstein's spontaneous coefficients in case of pure and doped ZnSe nanophosphors varies from 0.0033 to 0.2040 s^{-1} (Table-1). The Einstein's stimulated coefficients in case of pure and doped ZnSe nanophosphors varies from 0.126×10^{16} to 6.343×10^{16} m^3(rad/s)/(J/s) (Table-2). The oscillator strength which contribute significantly to the luminescence, range from 0.061×10^{-5} to 4.300×10^{-5} (Table 3). The integrated cross-section values (Table-3) vary from 0.024×10^{-9} to 1.831×10^{-9} m^2s^{-1}. The dipole moment values (Table-4) varies from 0.656×10^{-31} to 4.755×10^{-31} Cm. These values don't show any appreciable trend with variation of impurity concentration and the emission wavelength also don't show much change with impurity concentration as blue emission is observed for all the samples.

6. Conclusions

ZnSe nanoparticles are fabricated by using chemical precipitation technique and confirmation of size is done by XRD and TEM studies. Laser induced photoluminescence behaviour is used to calculate various optical parameters such as Einstein's spontaneous coefficients, Einstein's stimulated coefficients, oscillator strengths, integrated cross-section and dipole moments in these nanostructures.

Acknowledgement

This research work has been supported by Department of Science and Technology(DST), New Delhi through major Research Project No. SR/S2/CMP/02/2005 dated May, 2006. The financial support by DST is gratefully acknowledged.

References

[1] Lehmann, W, Journal of Luminescence **5**, 87 (1972).
[2] Ronda, C R, Journal of Alloys & Compounds, **225**, 534 (1995).
[3] Choi, H; Kim, C H; Pyun, C H and Kim, S J, Journal of Solid State Chemistry, **138,** 149 (1998).
[4] Kravets, V G, Journal of Optical Materials, 16 (2001) p369.
[5] Khare, R P; BhaskerRaj, C D and Sebastian, T B, Indian Journal of Pure & Applied Physics, **23**, 102 (1995).
[6] Yamura, Y and Shibukawa, A, Japanese Journal of Applied Physics, Part 1 (Regular Papers & Short Notes), **32**(7), 3187 (1993).
[7] Yang, P; Lu, M; Xu, D. Yaun, D; Song, C and Zhou, G, Journal of Physics & Chemistry of Solids, **62**, 1181 (2001).
[8] Harris, T D, Tytle, F E, Ultrasensitive Laser Spectroscopy, Academic Press Inc., New York, (1983).
[9] Ali, A. W, Kolb, AC and Anderson, A D, Journal of Applied Optics, **6**, 2115 (1967).
[10] Smith, P W; Duguay, M A and Ippen, E P, Progress in Quantum Electronics, Pergamon Press, Oxford, (1974).

[11] Demtroder, W, Laser Spectroscopy: Basic Concepts and Instrumentation, Springer Verlag, New York, (1988).
[12] Carlin, P B; Bennet Jr, W R, Journal of Applied Optics, **15**, 2020 (1976).
[13] Chan, Ch K, Laser Technical Bulletin, Spectra Physics, **8**, 20 (1978).
[14] Hartig P R; Sauer, K; Lo, G C and Laskovar, B, Review of Scientific Instruments **47,** 1122 (1976).
[15] Lewis, C; Ware, W R; Doemney, L J and Nemzek, T L, Review of Scientific Instruments, **44,** 107 (1973).
[16] Randall, J T & Wilkins, M H F, Proceedings Regional Society, London, Service A **184**, 390 (1945).
[17] Bube, R H, Physical Review **80**, p655 (1950).
[18] Jain, K L and Ranade, J D, Indian Journal of Physics, **48**, 1080 (1974).
[19] Bhatti H S, Nair N U V and Singh R D, Indian J Pure & Appl Phys, **20**, 5 (1982).
[20] Kothandaraman C, Kuskosky I, Neumark G F and Park R M, Appl. Phys. Lett. **69**(11), 1523 (1996).
[21] Suyver J F, Wuister S F, Kelly J J and Meijerink A, Phys. Chem. Chem. Phys. **2**, 5445 (2000).
[22] Thaddeus J Norman Jr., Maganr D, Bridges F and Zhang Jin Z, Mat. Res. Soc. Symp. Proc. Material Research Society (USA). 776 (2003).
[23] Changlong Jiang, Wangqun Zhang, Guifu Zou and Weicao Yu, Nanotech. **16**, 551 (2005).
[24] Shan C X, Liu Z, Zhang, X.T, Wong C C and Hark S K, Nanotech. **17**, 5561 (2006).
[25] Venkatachalam S, Mangalaraj D and Narayandass Sa K, J. Phys. D: Appl. Phys. **39,** 4777 (2006).
[26] Lehmann W and Rayan F M, Journal of Electrochemical Society **118**, 477 (1971).
[27] Kuhl J, Klingenberg H and Vonder Linde P, Journal of Applied Physics, **18**, 279 (1979).
[28] Gupta C S, Indian Journal of Pure & Applied Physics **37**, p906 (1999).
[29] Gupta C S, Indian Journal of Pure & Applied Physics **38,** 821 (2000).
[30] Gupta C S, Indian Journal of Physics, **75A**(5), 535 (2001).
[31] Kaeble E F, Handbook of X-rays, McGraw-Hill, New York, 1967.